

Fast-Ion Losses due to High-Frequency MHD Perturbations in the ASDEX Upgrade Tokamak

M. García-Muñoz,^{1,*} H.-U. Fahrbach,¹ S. Günter,¹ V. Igochine,¹ M. J. Mantsinen,^{1,4} M. Maraschek,¹ P. Martin,^{2,3}
P. Piovesan,^{2,3} K. Sassenberg,^{1,5} and H. Zohm¹

¹Max-Planck-Institut für Plasmaphysik, EURATOM Association Boltzmannstrasse 2, D-85748 Garching, Germany

²Consorzio RFX, Associazione EURATOM-ENEA per la fusione, Padova, Italy

³Physics Department, University of Padova, Italy

⁴Helsinki University of Technology, Association Euratom-Tekes, P.O. Box 4100, FIN-02015 HUT, Finland

⁵University College Cork, Association EURATOM-DCU, Cork, Ireland

(Received 24 June 2007; published 6 February 2008)

Time-resolved energy and pitch angle measurements of fast-ion losses correlated in frequency and phase with high-frequency magnetohydrodynamic perturbations have been obtained for the first time in a magnetic fusion device and are presented here. A detailed analysis of fast-ion losses due to toroidal Alfvén eigenmodes has revealed the existence of a new core-localized magnetohydrodynamic perturbation, the *sierpes* mode. The *sierpes* mode is a non-Alfvénic instability which dominates the losses of fast ions in ion cyclotron resonance heated discharges, and it is named for its footprint in the spectrograms (“*sierpes*” means “snake” in Spanish). The *sierpes* mode has been reconstructed by means of highly resolved multichord soft-x-ray measurements.

DOI: 10.1103/PhysRevLett.100.055005

PACS numbers: 52.55.Fa, 52.25.Xz, 52.35.Bj, 52.55.Pi

In fusion plasma devices, it is necessary that fast (i.e., suprathreshold) ions generated by heating systems and fusion born α particles are well confined until they transfer their energy to the plasma. Magnetohydrodynamic (MHD) instabilities can be driven by a population of fast ions and/or they can lead to an enhancement of the fast ions radial transport. Significant losses of these ions may reduce the heating as well as the neutral beam injection (NBI) current drive efficiency [1]. In addition, loss of fast ions that is sufficiently intense and localized may cause damage to plasma facing components in the vacuum vessel. This is especially important in large fusion devices like the International Tokamak Experimental Reactor (ITER) where even a small fraction of lost energetic ions might be intolerable [2]. Moreover, the study of the fast-ion physics in high β_{fast} (fast-ion pressure divided by magnetic pressure) discharges is important also to understand the formation of internal transport barriers (ITBs) [3], and in general the plasma MHD stability [4].

Fast-ion driven instabilities like toroidal Alfvén eigenmodes (TAEs) are extensively studied theoretically [5] and experimentally [6] in magnetic fusion devices. In general, the interaction of energetic particles with Alfvén waves can be described by the properties of the background plasma; however, when there is a sufficiently large energetic particle population, these particles can alter the plasma characteristics. As a result, new modes of a shear Alfvénic character [energetic particle modes (EPMs)] arise. Losses of fast ions due to TAEs [7,8] and EPMs [9,10] have been reported in many conventional aspect ratio tokamaks. However, these studies are either based on neutron drops correlated with bursting MHD instabilities or are lacking of the necessary time-resolved pitch angle and energy measurements of the lost ions.

In this Letter, we present the first time-resolved energy and pitch angle measurements of fast-ion losses correlated in frequency and phase with TAEs. The fast-ion loss detector (FIL) [11] design is based on the concept of the α -particle detector used for the first time in TFTR [12] and more recently in other major fusion devices like CHS [13], W7-AS [14], LHD [15], and JET [16]. The very high time resolution of the measurements (1 MHz bandwidth) has allowed to identify a new core-localized MHD perturbation, the *sierpes* mode (“*sierpes*” translates to “snake”), in the ASDEX Upgrade (AUG) tokamak [17]. The radial eigenfunction of TAEs and *sierpes* modes have been measured with the high resolution multichord soft x-ray (SXR) diagnostic [18].

The experiments have been mainly performed in plasmas with toroidal plasma current $I_p = 1.0\text{--}1.2$ MA, toroidal field $B_t = 2.0\text{--}2.2$ T, safety factor at the edge $q_{95} = 3.2\text{--}4.0$, and ion cyclotron resonance heating (ICRH) as main heating and fast particle source. 5 MW of on axis ICRH of hydrogen minority was applied in a deuterium plasma ($n_H/n_D \approx 6\%$). Figure 1(a) shows the typical core line integrated electron density, n_e , together with ICRH power for a reference discharge, No. 21 083. Figures 1(b) and 1(c) show, respectively, the Fourier spectrogram for a magnetic fluctuation signal and for a SXR signal, corresponding to a line of sight passing through the plasma core. Several dominant frequencies are visible between 150 and 225 kHz. They correspond to TAEs with different toroidal mode numbers [19] n 's ($n = 3, 4, 5, 6, 7$), whose presence is confirmed also by comparison with linear resistive MHD calculations carried out with the CASTOR code [20]. At lower frequencies, up to 25 kHz, some bursting fishbone modes appear. Fishbones are broadly known as a fast particle driven ($m = l, n = 1$)

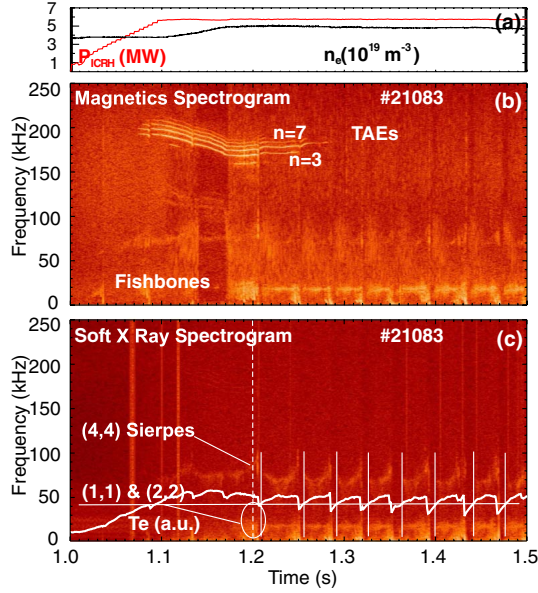


FIG. 1 (color online). AUG discharge 21083: (a) core line integrated electron density (n_e) and total ICRH power (P_{ICRH}). (b) Spectrogram of an in-vessel magnetic pickup coil. (c) Spectrogram of a core SXR channel. The local core electron temperature (T_e) indicating the mode occurrence threshold is superimposed in white. The vertical white dashed line indicates the time at which the mode structure analysis was done.

MHD perturbation with m the poloidal mode number [19]. An interesting feature is present in the SXR spectrogram at intermediate frequencies, ~ 80 kHz, where a dominant pattern emerges. We call this new plasma perturbation the sierpes mode because of its footprints in the fast-ion loss spectrogram and the fact that it is hardly visible for the Mirnov pickup coils [21].

The sierpes mode is more weakly dependent on plasma parameters than the TAEs, remaining unstable usually for time periods much longer than the TAEs, eventually up to 1 sec, and it is unaffected by changes in the magnetic safety factor, q profile [19]. In fact, the frequency of the sierpes mode does not change with the toroidal magnetic field B_t or the core electron density n_e . A rapid change of the electron density, n_e , due to low- (L) to high- (H) mode confinement transition (see Fig. 1) is followed by a change in the TAE frequency, as expected, but not by a change in the sierpes mode frequency. This hints that the sierpes mode is not an Alfvénic mode. Furthermore, the rapid frequency rise before the sawtooth crashes [19] cannot be explained by the classical Alfvénic physics since no relevant plasma parameter (i.e., n or B_t) can change so fast. In fact, the behavior before the sawtooth crash suggests some kinetic effects of the energetic particles as in the EPM case.

Figure 1(c) also shows the electron temperature, T_e , near the plasma center measured by the electron-cyclotron-emission (ECE) diagnostic. A strong dependence of the sierpes mode occurrence on the local T_e is observed. The sierpes mode appears always above a threshold in the local electron temperature, which is approximately $T_e =$

1.9 keV in the present conditions [the threshold is indicated in Fig. 1(c) by the horizontal line]. The mode always disappears at the sawtooth crashes and appears again within the next ≈ 10 ms, when the T_e , i.e., the collisionality (ν_e), has reached the threshold. It is important to note that the sierpes mode has been found with the same characteristics in both L- and H-mode confinement discharges.

The toroidal, n , and poloidal, m , mode numbers of the sierpes mode ($m = 4$, $n = 4$) were obtained from Mirnov loops and SXR measurements along different lines of sight, respectively.

The TAE and sierpes mode internal structure is reconstructed by means of highly resolved multichord SXR measurements which images the SXR radiation emitted by the plasma. The magnitude of the SXR fluctuation due to the $n = 4$ TAE and sierpes mode is extracted for all lines of sight by cross correlation with the FILD channel No. 13, which detects losses from both modes [see its Fourier spectrogram in Fig. 4(b)]. The magnetic field line radial displacement associated with the two modes is computed by dividing the SXR fluctuation profiles by the local gradient of the SXR brightness profile. Figure 2(a) shows that the displacement profile of the dominant TAE ($n = 4$) is fairly localized in radius ($\Delta\rho_{\text{pol}} \approx 0.3$) and located at about mid radius, with a maximum at $\rho_{\text{pol}} \approx 0.55$. The maximum TAE displacement ranges from 0.1 to 0.4 mm and the inferred core magnetic perturbation amounts to $\delta b_r/B_t = k_{\parallel}\psi_r = 0.2\text{--}5 \times 10^{-4}$. The sierpes mode [Fig. 2(b)] has a more core-localized eigenfunction, which is peaked around $\rho_{\text{pol}} \approx 0.25$ and it extends up to $\rho_{\text{pol}} \approx 0.5$, leading to a maximum displacement of the order of 0.5 mm in the plasmas analyzed so far. It is interesting to note that there is a radial region, $\rho_{\text{overlap}} \in (0.2, 0.5)$, where the $n = 4$ TAE and sierpes eigenfunctions overlap with nonzero values.

The radial position and radial width of the measured TAE eigenfunctions are reasonably consistent with those predicted by the CASTOR code, Figs. 2(c) and 2(d). To compare the experimental profiles with theoretical predictions, the MHD interpretation code (MHD-IC) was used to simulate the SXR signals with theoretical eigenfunctions as input [22]. CASTOR eigenfunctions were used to simulate the TAE profiles, Fig. 2(e). For the sierpes mode, lacking at present a theoretical model of it, a simple analytic Gaussian eigenfunction centered at $\rho_{\text{pol}} \approx 0.25$, as shown in Fig. 2(f), was used that best fits the sierpes experimental displacement. Figure 2(b) also shows the fast proton pressure profile as calculated with the ICRH modeling code PION [23] for discharge No. 21083. The volume averaged fast proton beta, β_{fast} , of $\approx 0.3\%$ as given by PION is about 25% of the volume averaged total plasma beta, and the dimensionless fast proton pressure gradient $|R\nabla\beta_{\text{fast}}|$ is in the range of 0.01— 0.04 at $\rho_{\text{pol}} \in (0.2, 0.5)$ where the TAE and sierpes modes are localized. The calculated ratio of fast proton density to electron density, the average perpendicular tail energy of protons, and the fast proton

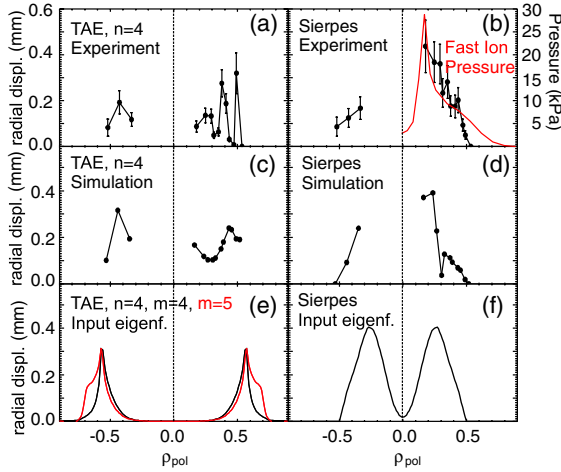


FIG. 2 (color online). AUG discharge 21083: (a)–(b) radial displacement of the $n = 4$ TAE and the sierpes mode, respectively, obtained from SXR, together with the fast proton pressure profile as given by the PION code; (c)–(d) show the same quantities modeled with the MHD-IC code; (e)–(f) radial eigenfunctions used as inputs to the MHD-IC code.

beta attain the peak value of 5.5%, 130 keV, and 1.7%, respectively, at $\rho_{pol} \approx 0.2$ in the close vicinity of the ion cyclotron resonance.

Figure 3 shows a CCD frame for the discharge No. 21011 at $t = 1.43$ s where both TAEs and sierpes are present. Two different contributions to the fast-ion loss pattern are simultaneously visible at different gyroradii and almost the same pitch angle. For the magnetic field at the probe $B_t = 1.6$ T, the losses peaked at gyroradius of 45 mm and pitch angles between 68° – 70° correspond to hydrogen ions at energies of ≈ 250 keV. The losses at higher gyroradii appear with a much broader distribution in giroradii; between 60 and 110 mm correspond to hydrogens with $E_H \approx 1$ MeV and pitch angles between 62° and 68° . During the experiments presented here the detector head front side was 5 mm in the limiter shadow.

In order to identify the MHD perturbations responsible for these losses, a fast Fourier transformation (FFT) was applied to the signal of the photomultipliers which observe the phase space regions where losses are detected. Figure 4(a) shows the spectrogram of a signal, which is measuring lost ions with a gyroradius ≈ 45 mm (upper spot in Fig. 3). The spectrogram in Fig. 4(b) refers to ion losses at higher gyroradii (60–110 mm), i.e., the larger spot in Fig. 3. A clear correlation between the TAE frequency pattern and the fast-ion loss frequencies is observed in both spectrograms. In addition, the frequencies of the sierpes mode, at around 80 kHz, emerge with a dominant character in the fast-ion loss pattern [Fig. 4(b)], lasting for a longer time. Tracking the frequencies corresponding to the individual TAEs $n = 4$ and $n = 6$ in both FILD spectrograms, we observe stronger TAE losses (up to a factor of 3 higher) if the sierpes mode is also ejecting fast ions. Figure 4(c) shows the temporal evolution of the losses at $n = 4$ and

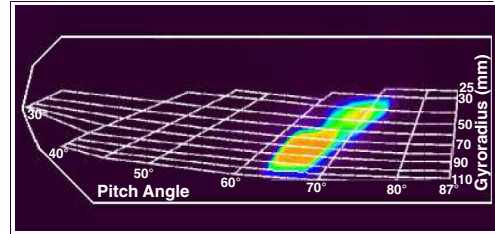


FIG. 3 (color online). AUG discharge 21011: CCD view of the light pattern produced by the incident ions ejected from the plasma due to interactions with high-frequency modes.

$n = 6$ TAE frequencies without sierpes losses (red lines) and with sierpes losses (black lines). The overlapping of the radial eigenfunctions might be the reason for this, by channeling the ions which fulfill the loss conditions from the plasma core to the edge. The high temporal resolution of FILD has allowed to identify the phase correlation between the TAE magnetic perturbation and its fast-ion losses, see Fig. 4(d). The relative toroidal and poloidal location of FILD with respect to the magnetic pickup coil used for the phase analysis is $(d\phi, d\theta) = (0.27, 0.08)$ rad.

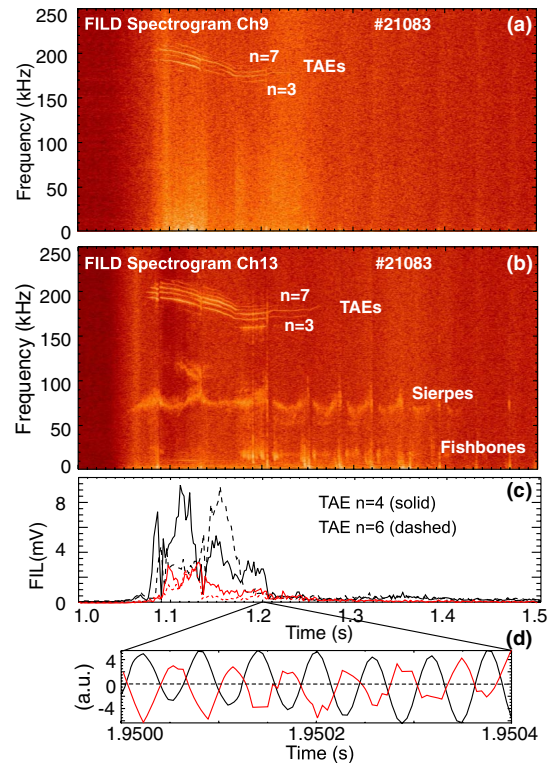


FIG. 4 (color online). AUG discharge 21083: (a) spectrogram of the photomultiplier signal which is covering the area at lower energies (i.e., smaller gyroradii). (b) Spectrogram of the photomultiplier signal at higher energies (i.e., larger gyroradii). (c) Fast-ion loss signal at TAE $n = 4$ and $n = 6$ frequencies with curves from panel (a) in red and from panel (b) in black. (d) Phase correlation between TAE magnetic perturbation (black line) and losses (red line).

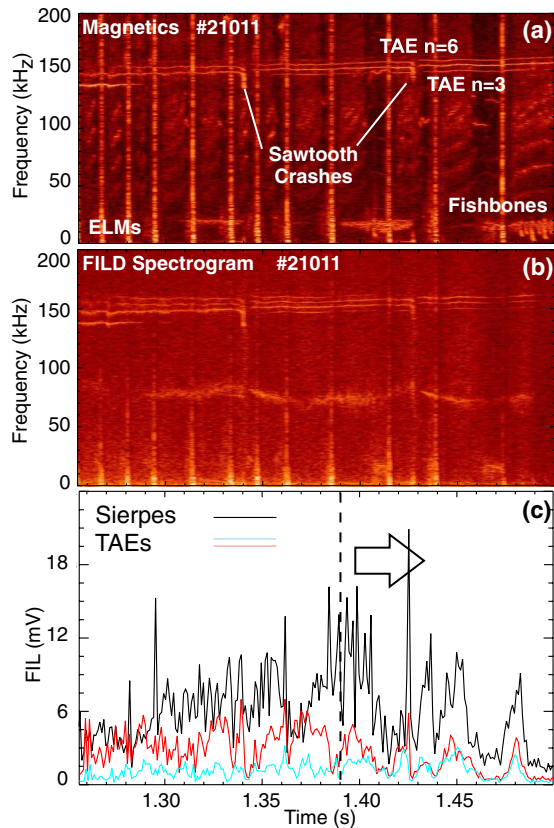


FIG. 5 (color online). AUG discharge 21 011. (a) Spectrogram of an in-vessel magnetic pickup coil. (b) Spectrogram of a FILD channel showing fast-ion losses correlated with various types of MHD activities (ELMs, sawtooth, and fishbones) [19]. (c) Fast-ion loss (FIL) signal at TAE $n = 4$ and $n = 6$, and sierpes frequencies.

To compare the contribution to the loss pattern of the individual TAEs and sierpes mode, a time window has been selected in which they do not change strongly in frequency. Figures 5(a) and 5(b) show, respectively, the spectrograms of the magnetic fluctuation and of one FILD channel during that time window. We track the frequencies of the TAEs, $n = 4$ and $n = 5$, and of the sierpes mode in the fast-ion loss spectrogram and extract their amplitudes, as shown in Fig. 5(c). Although each magnetic perturbation is ejecting ions during the entire time window, it is obvious that the fast-ion losses at the sierpes frequency are stronger than the TAEs-induced fast-ion losses. The correlation in the occurrence of the spikes from $t = 1.39$ s on in Fig. 5(c) gives further evidence for a coupling between either plasma perturbations [24] or fast-ion loss mechanisms. However, the frequency behavior of the magnetic perturbation for both modes reveals no coupling between magnetic perturbations; as a consequence, only the losses are connected. The more virulent effect of the sierpes mode on the fast-ion population might be explained on the basis of a broader loss condition. A Fourier power spectrum at $t \sim 1.35$ s, from Fig. 5(b), gives the frequency width of the peaks corresponding to the losses due to each MHD mode.

The peak of the fast-ion losses induced by the sierpes mode appears at 75 kHz with a full width at half maximum (FWHM) of up to 10 kHz while the peaks corresponding to the individual TAE losses have a FWHM of up to 2 kHz.

In summary, we have obtained for the first time energy and pitch angle measurements of fast-ion losses correlated in frequency and phase with high-frequency modes. Selective TAE-induced fast-ion losses, as expected from the theory, have been observed in ICRH heated discharges. A new MHD perturbation, called sierpes mode, has been identified due to its strong influence on the energetic ion losses. Sierpes-mode-induced fast-ion losses usually are stronger than those induced by TAEs. Core density changes due to (L-H)-mode transitions have revealed the non-Alfvénic character of the sierpes mode. Sierpes as well as TAE eigenfunctions have been measured. A spatial overlapping of their eigenfunctions leads to a fast-ion loss coupling and shows the strong influence that a core-localized fast-ion driven perturbation may have on the fast-ion population. These results represent a breakthrough for the use of scintillator based detectors for diagnosing energetic ion losses in fusion plasmas.

The authors wish to acknowledge the support of J. Snipes, A. Fasoli, D. Borba, S.-D. Pinches, and P. Lauber for the very fruitful discussions.

*Manuel.Garcia-Munoz@ipp.mpg.de

- [1] C. B. Forest *et al.*, Phys. Rev. Lett. **79**, 427 (1997).
- [2] W. W. Heidbrink and G. J. Sadler, Nucl. Fusion **34**, 535 (1994).
- [3] K. L. Wong *et al.*, Nucl. Fusion **45**, 30 (2005).
- [4] N. N. Gorelenkov *et al.*, Nucl. Fusion **43**, 594 (2003).
- [5] G. Y. Fu and J. W. Van Dam, Phys. Fluids B **1**, 1949 (1989).
- [6] K. L. Wong, Plasma Phys. Controlled Fusion **41**, R1 (1999).
- [7] H. H. Duong *et al.*, Nucl. Fusion **33**, 749 (1993).
- [8] D. Darrow *et al.*, Nucl. Fusion **37**, 939 (1997).
- [9] S. Bernabei *et al.*, Phys. Plasmas **6**, 1880 (1999).
- [10] M. Isobe *et al.*, Nucl. Fusion **46**, S918 (2006).
- [11] M. García-Munoz *et al.*, Nucl. Fusion **47**, L10 (2007).
- [12] S. J. Zweben, Nucl. Fusion **29**, 825 (1989).
- [13] M. Isobe *et al.*, Rev. Sci. Instrum. **70**, 827 (1999).
- [14] A. Werner and A. Weller *et al.*, Rev. Sci. Instrum. **72**, 780 (2001).
- [15] M. Nishiura *et al.*, Rev. Sci. Instrum. **75**, 3646 (2004).
- [16] S. Baeumel *et al.*, Rev. Sci. Instrum. **75**, 3563 (2004).
- [17] A. Herrmann and O. Gruber, Fusion Sci. Technol. **44**, 569 (2003).
- [18] A. Mueck, Ph.D. thesis, Technical University of Munich, 2004.
- [19] J. A. Wesson, *Tokamaks* (Clarendon Press, Oxford, 1997).
- [20] W. Kerner *et al.*, J. Comput. Phys. **142**, 271 (1998).
- [21] M. Schittenhelm and H. Zohm, Nucl. Fusion **37**, 1255 (1997).
- [22] V. Igoshina *et al.*, Nucl. Fusion **43**, 1801 (2003).
- [23] L.-G. Eriksson *et al.*, Nucl. Fusion **33**, 1037 (1993).
- [24] N. A. Crocker *et al.*, Phys. Rev. Lett. **97**, 045002 (2006).